The Aβ 3-Pyroglutamyl and 11-Pyroglutamyl Peptides Found in Senile Plaque Have Greater β-Sheet Forming and Aggregation Propensities in Vitro than Full-Length Aβ[†]

Weilan He and Colin J. Barrow*

School of Chemistry, The University of Melbourne, Parkville, Victoria 3052, Australia

Received March 11, 1999; Revised Manuscript Received May 24, 1999

ABSTRACT: Aβ isolated from neuritic plaque and vascular walls of the brains of patients with Alzheimer's disease has been shown to contain significant quantities of Aβ peptides which begin at residue ^{3}Glu or ^{11}Glu in the form of pyroglutamyl residues (Aβ3pE and Aβ11pE). To investigate the effects of these N-terminal modifications on the biophysical properties of Aβ, peptides Aβ1−40, Aβ3pE−40, Aβ11pE−40, Aβ1−28, Aβ3pE−28, and Aβ11pE−28 were synthesized. Using circular dichroism spectroscopy, we determined that the pyroglutamyl-containing peptides form β-sheet structure more readily than the corresponding full-length Aβ peptides, both in aqueous solutions and in 10% sodium dodecyl sulfate micelles. Trifluoroethanol spectra indicated that the relative β-sheet to α-helical stability is higher for the pyroglutamyl-containing peptides. Sedimentation experiments show that the pyroglutamyl-containing peptides have greater aggregation propensities than the corresponding full-length peptides. Comparison between the Aβ40 and the Aβ28 series indicated that the greater β-sheet forming and aggregation propensities of the pyroglutamyl peptides are not simply due to an increase in hydrophobicity.

Alzheimer's disease (AD)[1] is a neurodegenerative disorder characterized pathologically by the progressive deposition of amyloid-β peptide (Aβ) both intraneuronally and extracellularly in the brain (*1*). The extracellular deposits include amyloid senile plaque and cerebrovascular amyloid (*2*, *3*). The deposition of amyloid appears to be a critical factor in disease development, and Aβ itself appears to be neurotoxic (*4*, *5*). Aβ is derived proteolytically from the Aβ precursor protein (APP) in generating mainly two Aβ forms, Aβ1−40 and Aβ1−42, which differ in the position of their C-terminal cleavage from APP. APP has a single membrane-spanning domain near its C-terminus. Within APP, Aβ spans the extracellular space−membrane interface, with the N-terminal 28 amino acid residues on the outside of the cell and the C-terminal residues within the hydrophobic domain (*6*). Both Aβ1−40 and Aβ1−42 have been widely studied in efforts to determine the influence of factors such as pH on their ability to form the β-sheet structure of amyloid (*7*−*9*), their relative depositability (*10*), and neurotoxicity (*11*). All the charged residues in the Aβ sequence fall within the 28 N-terminal residues, and it is this region that makes the Aβ peptide conformationally sensitive to external influences such as pH and ionic strength, and is probably the region involved in binding to both metals and other proteins (*7*).

A number of N-terminally modified Aβ species have recently been identified in the amyloid of AD patients. These modifications include isomerization of aspartic acid 1 and 7 (*12*−*15*) and pyroglutamate formation (*11*, *14*−*19*). In fact, the major component of AD senile plaque may not be full-length Aβ, but instead N-terminally modified Aβ, beginning at glutamate 3 and post-translationally modified through intramolecular dehydration to contain an N-terminal pyroglutamate (*14*, *16*, *17*). Pyroglutamyl forms of Aβ, termed Aβ3pE and Aβ11pE here, were shown to constitute more than 50% of the Aβ in neuritic plaque in some individuals. The loss of three charges, including an N-terminal charge, for Aβ3pE, and six charges for Aβ11pE, could have a significant effect on the conformational behavior and depositability of these peptides. In addition, the N-terminal pyroglutamate would be expected to offer some protection against in vivo proteolysis of these peptides, increasing their importance as potential seeds for amyloid formation (*17*). Such decreased protease susceptibility has been observed previously for aspartic acid isomerization forms of Aβ found in AD amyloid (*20*).

To examine the effects of N-terminal pyroglutamate formation on the conformation and depositability of Aβ, we have synthesized Aβ1−40, Aβ3pE−40, Aβ11pE−40, Aβ1−28, Aβ3pE−28, and Aβ11pE−28 (Figure 1). The relative β-sheet forming propensities of these peptides were investigated using circular dichroism (CD) in aqueous solution and in sodium dodecyl sulfate (SDS) micelles. The influence of pH on the conformation of each peptide was also investigated. The ability of trifluoroethanol (TFE) to induce

[†]This work was funded by the Australian Research Council and by a SUNBOR grant from the Suntory Institute for Bioorganic Research.

* To whom correspondence should be addressed: School of Chemistry, The University of Melbourne, Parkville, Victoria 3052, Australia. Phone: +61-3-9344-6484. Fax: +61-3-9347-5180. E-mail: c.barrow@chemistry.unimelb.edu.au.

[1] Abbreviations: Aβ, amyloid β-peptide; AD, Alzheimer's disease; Glu, glutamic acid; Aβ3pE, 3-pyroglutamyl Aβ; Aβ11pE, 11-pyroglutamyl Aβ; SDS, sodium dodecyl sulfate; APP, Aβ precursor protein; CD, circular dichroism; HBTU, 2-(1*H*-benzotriazol-1-yl)-1,1,3,3-tetramethyluronium hexafluorophosphate; HOBt, 1-hydroxybenzotriazole; DIPEA, diisopropylethylamine; HFIP, 1,1,1,3,3,3-hexafluoro-2-propanol; HPLC, high-performance liquid chromatography; TFA, trifluoroacetic acid; TFE, trifluoroethanol; DS, Down's syndrome.

10.1021/bi990563r CCC: $18.00
Published on Web 08/17/1999

^{1}DAEFRHDSGYEVHHQKLVFFAEDVGSNKGAIIGLMVGGVV^{40}
^{3}pyroEFRHDSGYEVHHQKLVFFAEDVGSNKGAIIGLMVGGVV^{40}
^{11}pyroEVHHQKLVFFAEDVGSNKGAIIGLMVGGVV^{40}
^{1}DAEFRHDSGYEVHHQKLVFFAEDVGSNK^{28}
^{3}pyroEFRHDSGYEVHHQKLVFFAEDVGSNK^{28}
^{11}pyroEVHHQKLVFFAEDVGSNK^{28}

FIGURE 1: One-letter code sequences for the peptides synthesized during this study.

an α-helical conformation for each peptide was determined as an indication of relative α-helix to β-sheet stability. Relative aggregation propensities for these peptides were then determined using sedimentation.

MATERIALS AND METHODS

Peptide Synthesis. Peptides were synthesized using manual solid-phase Boc amino acid chemistry with in situ neutralization (*21*). Acylations were performed using 5 equiv of the Boc-protected amino acid, 4.9 equiv of 2-(1*H*-benzotriazol-1-yl)-1,1,3,3-tetramethyluronium hexafluorophosphate (HBTU), 5 equiv of 1-hydroxybenzotriazole (HOBt), and 7.5 equiv of diisopropylethylamine (DIPEA). Each acylation was monitored using ninhydrin monitoring (*22*), and couplings were repeated if necessary. Peptides were cleaved from the resin using anhydrous hydrogen fluoride with *p*-cresol and *p*-thiocresol as scavengers. After hydrogen fluoride removal, peptides were dissolved in trifluoroacetic acid (TFA) and precipitated with ether. Peptides were purified using an acetonitrile/water (0.01% TFA) gradient on a reverse-phase preparative Zorbax HPLC column heated to 60 °C. The peptide purity and identity were confirmed using analytical high-performance liquid chromatography (HPLC), electrospray mass spectrometry, and amino acid analysis.

Circular Dichroism Spectroscopy. CD spectra were obtained under a variety of solution conditions using a model 62DS CD spectropolarimeter (AVIV, Lakewood, NJ). The method that we used was similar to that previously described for Aβ (*8*). Briefly, peptide stock solutions were prepared in 1,1,1,3,3,3-hexafluoro-2-propanol (HFIP) for the Aβ40 series and acetonitrile in water (1:1) for the Aβ28 series. The concentrations of the stock solutions were determined using quantitative amino acid analysis. A known amount of this stock solution, normally 7 μL, was injected into 300 μL of the appropriate CD buffer directly in the 1 mm path length quartz cell. The solution was mixed and allowed to stand for 5 min before the spectrum was recorded. Measurements were taken at 0.5 nm steps over a 190−250 nm wavelength range; the baseline was subtracted, and the resulting spectra were smoothed.

Sedimentation Assay. The proportion of pelletable peptide was determined using a modified literature method (*23*). Briefly, peptide stock solutions were diluted to 50 and 100 μM in 50 mM sodium phosphate buffer at pH 5.0 and 7.2. The resulting diluted peptide solutions were separated into three equal portions and aliquoted into 1.5 mL microtubes. Each aliquot was incubated for 20 min, 3 h, and 24 h at room temperature. The solutions were then centrifuged for 10 min at 10 000 rpm. The ratio of peptide concentrations, as determined by fluorescamine assay, of the supernatant relative to noncentrifuged peptide was used to calculate the levels of sedimentation peptide. For the fluorescamine assay, a Molecular Devices f-max Fluorescence Microplate Reader with a 355 nm excitation wavelength filter and a 460 nm emission filter was used. All experiments were performed in triplicate with 250 μL samples in 96-well plates.

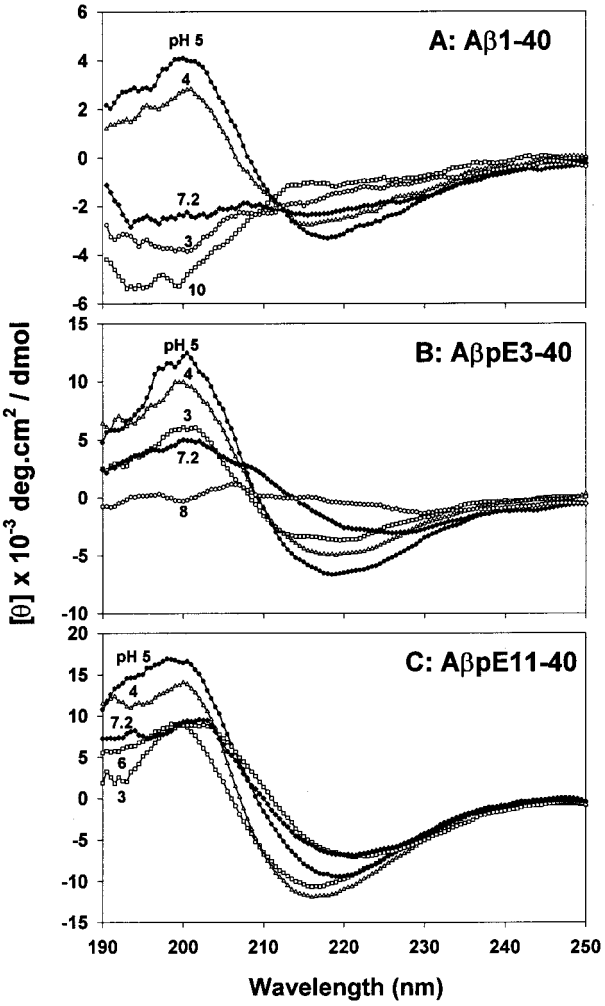

FIGURE 2: CD spectra showing the pH dependence of Aβ1−40 (A), Aβ3pE−40 (B), and Aβ11pE−40 (C) in aqueous phosphate-buffered solutions. Aβ3pE−40 and Aβ11pE−40 exhibit increased β-sheet content as compared to Aβ1−40. The number near each curve denotes the pH value at which that curve was obtained.

RESULTS

Influence of pH and SDS on the Conformation of Aβ1−40, Aβ3pE−40, and Aβ11pE−40. In aqueous solution at pH 7.2, Aβ1−40 is a mixture of random coil and β-sheet structure (Figure 2). At pH 4.0 and 5.0, the peptides becomes predominantly β-sheet, while at higher and lower pH values, the β-sheet structure is destabilized. Maximum β-sheet structure is observed at pH 5.0, which is consistent with what has been reported previously (*7*, *9*). The most obvious difference for the aqueous CD spectra of Aβ3pE−40 and Aβ11pE−40, as compared with that of Aβ1−40, is that the pyroglutamyl-containing peptides are mainly β-sheet at all pH values. The increased amount of β-sheet structure for both the Aβ3pE−40 and Aβ11pE−40, over that of Aβ1−40, is supported by significantly more intense minima close to 217 nm. Decreased random coil content is supported by the observation of no minima near 195 nm. Aβ3pE−40 has the most intense 217 nm minimum at pH 5.0, while the β-sheet minimum for Aβ11pE−40 is most intense at pH 4.0.

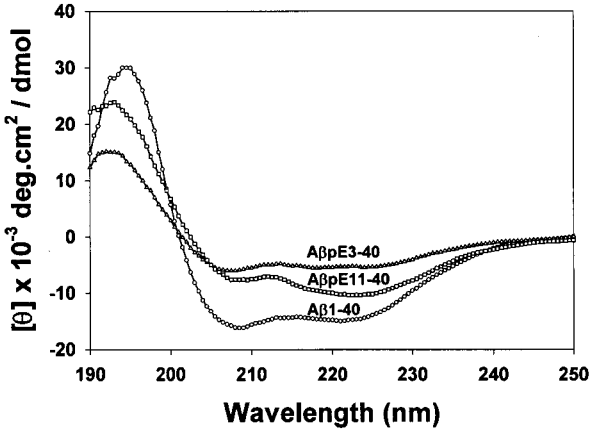

FIGURE 3: CD spectra of Aβ1−40, Aβ3pE−40, and Aβ11pE−40 in 10% SDS micelles at pH 5.0. Aβ3pE−40 and Aβ11pE−40 have lower α-helical content than does Aβ1−40.

In SDS micelles, all three peptides contain some α-helical structure, as determined by the presence of distinctive double minima close to 208 and 222 nm (*24*). On the basis of the molar ellipticities at 208 nm from the CD spectrum obtained at pH 7.2, the α-helical content of each peptide is 45, 24, and 36% for Aβ1−40, Aβ3pE−40, and Aβ11pE−40, respectively (data not shown) (*24*). The corresponding α-helical contents at pH 5.0 are 42, 10, and 11% for Aβ1−40, Aβ3pE−40, and Aβ11pE−40, respectively (Figure 3). At both pH 5.0 and pH 7.2, Aβ3pE−40 and Aβ11pE−40 have significantly lower α-helical content than does Aβ1−40, indicating lower helical stability for these pyroglutamate-containing peptides in SDS micelles.

To determine the relative β-sheet to α-helix stability, spectra were obtained in increasing amounts of TFE, a known α-helix-inducing solvent for Aβ (*8*). Aβ1−40 at pH 7.2 has a small β-sheet minimum with 10% TFE, but is predominantly α-helical with 20% or more TFE (Figure 4). This result is similar to that obtained for Aβ1−39 previously (*8*), is consistent with previous NMR and CD data obtained for Aβ1−40 (*25*−*27*), and indicates that the propensity of β1−40 peptide to form β-sheet at pH 7.2 is relatively low. This is consistent with the low amount of β-sheet observed for this peptide in aqueous solution at pH 7.2 (Figure 2). In contrast, Aβ3pE−40 is predominantly β-sheet at 20% TFE and is induced into α-helix at ≥30% TFE. The β-sheet structure of Aβ11pE−40 is even more stable, with this peptide remaining predominantly β-sheet at 30% TFE and not being induced into α-helix until the TFE level reaches ≥40% (Figure 4).

The Aβ1−42 peptide, which forms β-sheet structure much more readily than Aβ1−40, was previously shown to be predominantly β-sheet at 20% TFE and induced into α-helix at ≥30% TFE (*8*). These results indicate that Aβ3pE−40 has relative β-sheet to α-helix stability that is similar to that of Aβ1−42, while Aβ11pE−40 forms even more stable β-sheet structure. Both Aβ3pE−40 and Aβ11pE−40 form significantly more stable β-sheet structure at pH 7.2 than does Aβ1−40. At pH 5.0, all three peptides exhibited increased β-sheet stability compared to that at pH 7.2, and the order of β-sheet stability was as follows: Aβ11pE−40 > β3pE−40 > Aβ1−40 (results not shown).

Influence of pH and SDS on the Conformation of Aβ1−28, Aβ3pE−28, and Aβ11pE−28. Consistent with published

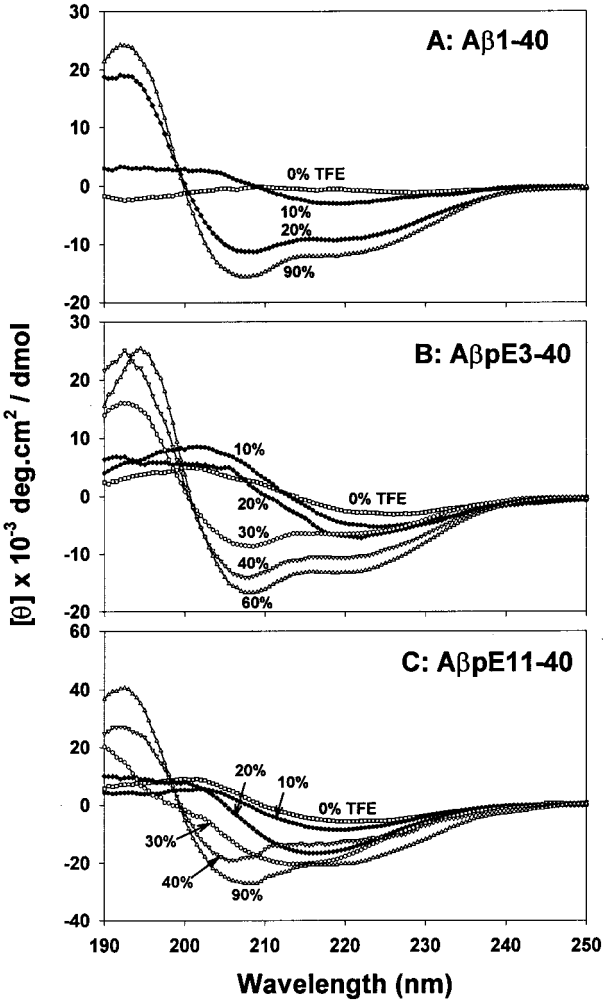

FIGURE 4: Relative stability of β-sheet to α-helix in the presence of the helix-inducing solvent TFE at pH 7.2, for Aβ1−40 (A), Aβ3pE−40 (B), and Aβ11pE−40 (C). Aβ1−40 is most readily induced into α-helix, Aβ3pE−40 intermediately, and Aβ11pE−40 least readily, indicating that N-terminal truncation and pyroglutamyl formation increase β-sheet stability relative to that of α-helix. The percentage of TFE that is used is denoted on the figure for each curve.

results for this peptide, Aβ1−28 is completely random coil at all pH values in aqueous solution, even after 24 h (*8*) (Figure 5). However, both Aβ3pE−28 and Aβ11pE−28 exhibit a decrease in the random coil 195 nm minima and an increase in the 217 nm β-sheet minima near pH 5.0. This is particularly noticeable for Aβ3pE−28, which has a clear β-sheet minimum at pH 5.0. This indicates that the pyroglutamyl-containing peptides have a propensity to form β-sheet structure in aqueous solution, even in the absence of the hydrophobic C-terminal residues.

In 10% SDS micelles, Aβ1−28 contains significant α-helix, with 208 and 222 nm minima observed at each pH (Figure 6 shows pH 5.0 data only). Interestingly, in contrast to that for Aβ1−40, helical content is increased rather than decreased for Aβ1−28 near pH 5.0, as compared to that at pH 7.2 (data not shown). This is probably because both α-helical and β-sheet structure are stabilized near pH 5.0, which is close to the isoelectric point of both peptides.[2] However, β-sheet structure predominates for the Aβ1−40 peptide, whereas for the Aβ1−28 peptide, which has a low propensity to form β-sheet structure, α-helix predominates.

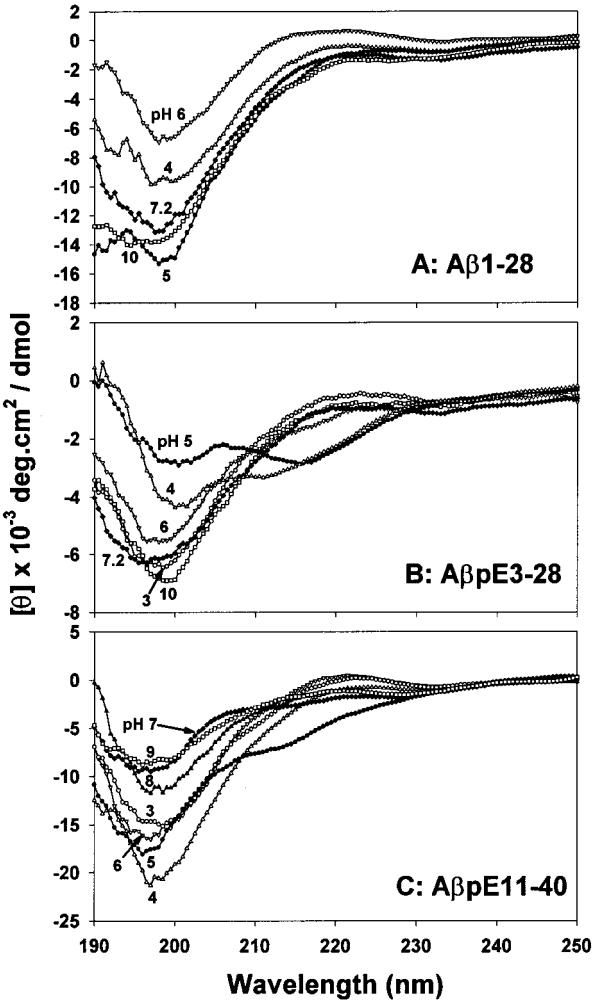

FIGURE 5: CD spectra showing the pH dependence of Aβ1−28 (A), Aβ3pE−28 (B), and Aβ11pE−28 (C) in aqueous phosphate-buffered solutions. Aβ1−28 is random coil at all pH values, while Aβ3pE−28 and Aβ11pE−28 exhibit some β-sheet structure near pH 5.0. The number near each curve denotes the pH value at which that curve was obtained.

The Aβ11pE−28 peptide gives spectra similar to those of Aβ1−28 at both pH 5.0 and 7.2, based on molar ellipticities. The CD spectra for Aβ3pE−28 near pH 7.2 and at more basic pH values are similar to those obtained for Aβ1−28. However, the CD spectra for Aβ3pE−28 at pH 4.0 and 5.0 in SDS micelles exhibit a clear β-sheet minimum at 220 nm, indicating that at these pH values this peptide is predominantly β-sheet, even in the presence of an SDS membrane-like environment (Figure 6 shows pH 5.0 data). Therefore, Aβ3pE−28, in particular, has a much greater β-sheet propensity than does Aβ1−28 in an acidic, hydrophobic membrane-like environment.

At both pH 5.0 and 7.2, Aβ1−28 is readily induced into an α-helical conformation by the addition of small amounts of TFE (*8*, *28*). Addition of 20% TFE induces significant helical content in Aβ1−28, which is maximized at close to 60% α-helix with ≥30% TFE (results not shown). Interestingly, in this study, we found that α-helix in Aβ1−28 was

[2] Using the program General Protein Mass Analysis for Windows (GPMAW) version 2.13, the isoelectric points are pH 5.2 for Aβ1−28 and −40, pH 6.2 for Aβ3pE−28 and −40, and pH 7.9 for Aβ11pE−28 and −40.

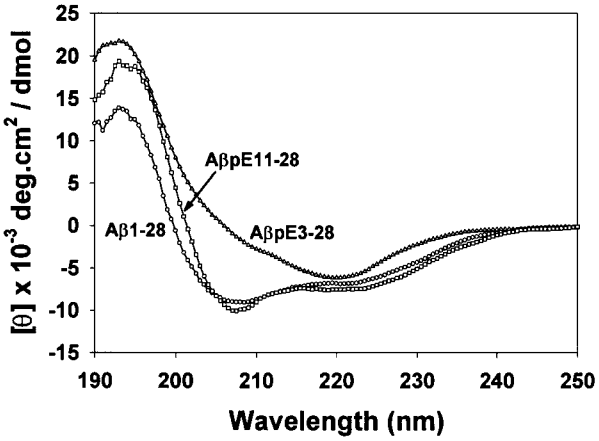

FIGURE 6: CD spectra of Aβ1−28, Aβ3pE−28, and Aβ11pE−28 in 10% SDS micelles at pH 5.0. Aβ3pE−28 forms mainly β-sheet structure, while Aβ1−28 and Aβ11pE−28 exhibit significant α-helical structure.

more stable at pH 5.0 than at pH 7.2, indicating that both α-helix and β-sheet are stabilized near pH 5.0, which is consistent with the results obtained in SDS micelles. In contrast to Aβ1−28, the pyroglutamyl peptides readily form β-sheet, rather than α-helix on the addition of TFE (Figure 7). For Aβ11pE−28, the β-sheet structure breaks down between 40 and 60% TFE, and α-helix predominates at 90% TFE. However, Aβ3pE−28 remains essentially β-sheet irrespective of the percentage of TFE. Both peptides exhibit more β-sheet structure at pH 5.0 than at pH 7.2, irrespective of the percentage of TFE added.

Comparison of the Aggregation Propensity of Aβ1−40, Aβ3pE−40, Aβ11pE−40, Aβ1−28, Aβ3pE−28, and Aβ11pE−28. The extent of sedimentation of each peptide was determined at pH values of 5.0 and 7.2, and at concentrations of 50 and 100 μM (50 μM data shown in Figure 8, 100 μM data not shown). At both pH values, each peptide exhibited time-dependent aggregation. Each peptide aggregated more rapidly at pH 5.0 than at pH 7.2 and at the higher concentration. The amount of sedimented peptide was similar for Aβ3pE−28 and Aβ11pE−28, with both peptides aggregating more extensively than Aβ1−28. For the Aβ1−40 series, the pyroglutamyl-containing peptides sedimented within 20 min at both concentrations and pH values, while Aβ1−40 aggregated much more slowly, with no detectable aggregation occurring in the first 20 min. These results indicate that N-terminal truncation and the pyroglutamyl group significantly increase the aggregation propensity of both Aβ1−28 and Aβ1−40.

DISCUSSION

For both the Aβ40 and Aβ28 series, the pyroglutamyl-containing N-terminal truncated peptides form β-sheet structure and aggregate more readily than the full-length forms. The pyroglutamyl peptides have an increased aggregation propensity in both aqueous solutions and SDS micelles. In addition, the increased aggregation propensity observed for Aβ3pE−28 and Aβ11pE−28 at pH 5 as compared with those at pH 7.2 (Figure 8), together with the increased β-sheet content of all peptides at pH 5 (Figures 2 and 5), indicates that acidolysis during Alzheimer's disease (*8*) may increase the extent of deposition not only of full-length Aβ but also of the pyroglutamyl forms. Also, the high

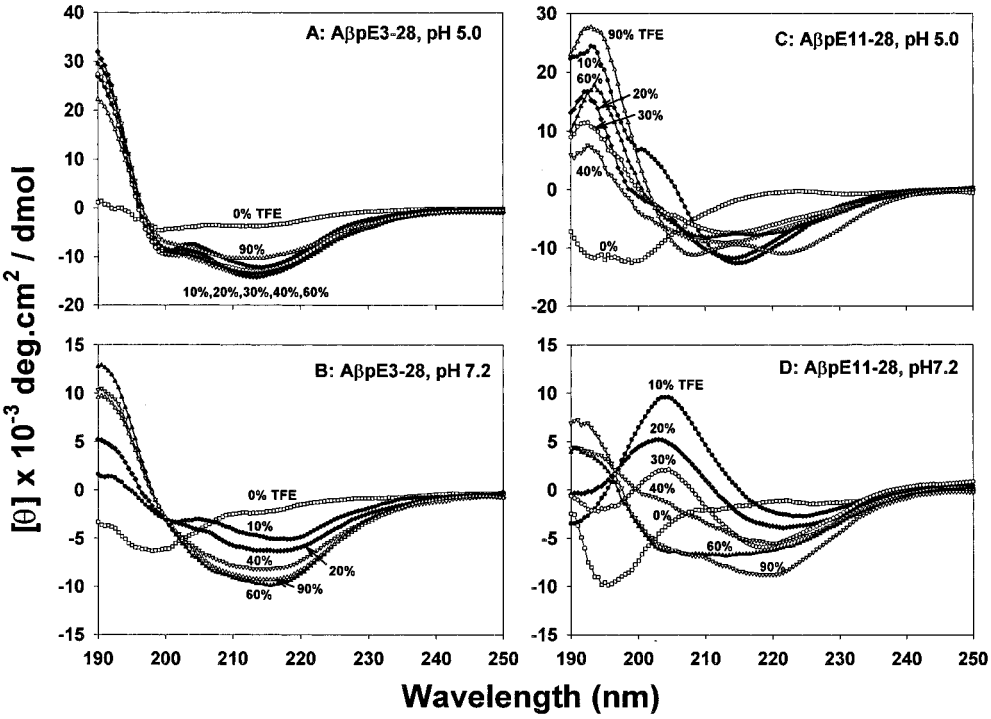

FIGURE 7: Relative stability of β-sheet to α-helix in the presence of the helix-inducing solvent TFE, for Aβ3pE−28 at pH 5.0 (A), Aβ3pE−28 at pH 7.2 (B), Aβ11pE−28 at pH 5.0 (C), and Aβ11pE−28 at pH 7.2 (D). Aβ1−28 is readily induced into α-helix (data not shown), while Aβ11pE−28 is helical only in 90% TFE. Aβ3pE−28 remained in a β-sheet conformation at all TFE concentrations. The β-sheet stability of Aβ3pE−28 and Aβ11pE−28 is greater at pH 5.0 than at pH 7.2, and neither peptide readily forms α-helical structure, in contrast to Aβ1−28 which readily forms helical structure in TFE (*7*). The percentage of TFE that is used is denoted on the figure for each curve.

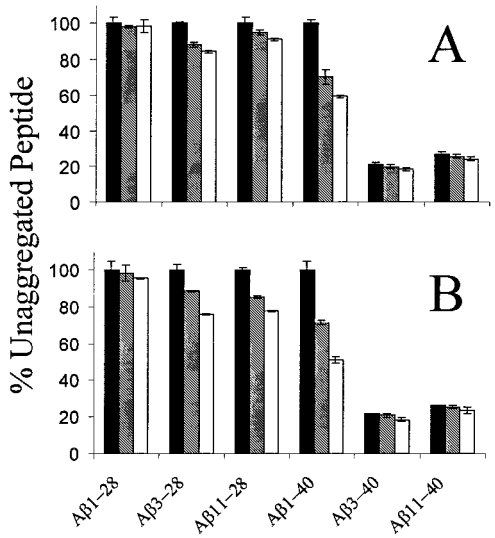

FIGURE 8: Time-dependent aggregation of 50 μM Aβ1−28, Aβ3pE−28, Aβ11pE−28, Aβ1−40, Aβ3pE−40, and Aβ11pE−40 as measured by fluorescamine assay of the nonsedimented to total peptide (100%) at pH 7.2 (A) and pH 5.0 (B), after 20 min (black bars), 3 h (hatched gray bars), and 24 h (white bars). Error bars represent the standard deviation from three repeat experiments. The pyroglutamyl-containing peptides aggregate significantly more rapidly than the full-length peptides.

aggregation propensities of both Aβ11pE−28 and Aβ11pE−40 indicate that the amino acid region between residues 11 and 28 is critical to aggregation and plays an important role in its pH dependence. The importance of this region for pH-dependent aggregation is also supported by previous reports where a peptide corresponding to residues 11−25 was shown to adopt β-sheet structure in aqueous solution (*28*), and deprotonation of acidic residues within this region promoted a helix−coil conformational transition in Aβ1−40 (*27*).

Although most studies of the aggregation behavior of Aβ have been performed with untruncated Aβ (Aβ1−40 or Aβ1−42), recent protein-chemical analyses of AD brain amyloid show that pyroglutamyl-containing forms of Aβ are major components of amyloid in both Down's syndrome (DS) and AD brain. For example, Aβ3pE has been reported to comprise 51% of Aβ in the neuritic plaques from nine AD brains (*14*). Also, Aβ3pE and untruncated Aβ are distributed in different areas of the brain, with the concentration of Aβ3pE plaques exceeding the concentration of untruncated Aβ plaques in frontal and temporal lobes (*17*). A recent quantitation of Aβ in the frontal cortex also identified Aβ3pE as the most abundant form (*16*). The different evolution of plaque in different brain regions indicates that Aβ3pE deposition probably preceded untruncated Aβ deposition in the course of plaque development. In addition, diffuse plaque contains mainly Aβ3pE, indicating that Aβ3pE rather than untruncated Aβ is present in the early stages of amyloid deposition (*17*). The second N-terminal pyroglutamyl form of Aβ, Aβ11pE, was identified as a minor component of plaque and diffuse amyloid in both DS and AD brain (*15*, *19*). The abundance of pyroglutamyl Aβ variants in both plaque core and diffuse plaque indicates that understanding the aggregation behavior of these peptides may be critical to investigations of amyloid formation in DS and AD. The results from our study indicating that pyroglutamyl peptides form β-sheet and aggregate more rapidly than full-length Aβ support the contention that these N-terminal modified peptides play a critical role in the early stage of amyloid formation in AD. The ability of these peptides to form fibrils

was not demonstrated in this study, although the determinant factor of Aβ fibrillogenesis is believed to be the secondary structure adopted by the peptide in its soluble state (*29*).

It has been proposed that both Aβ3pE and Aβ11pE, apparently present in all forms of DS and AD, may be unique forms present only in diseased brain as a result of impaired catabolism and clearance (*18*). These Aβ variants would be expected to be more protease resistant than untruncated Aβ, making them less readily cleared from the brain. Poor clearance, together with an increased aggregation propensity, could explain why the ratio of Aβ3pE to untruncated Aβ increases with age in DS brain. A similar explanation has been given for the increased abundance of aspartic acid-isomerized Aβ peptides found in AD-infected brain (*20, 30*). Our results clearly show that although both full-length and pyroglutamate-containing Aβ peptides will form monomeric α-helical structure in a hydrophobic membrane-like environment such as SDS micelles or TFE, the pyroglutamyl variants have a much greater tendency than full-length Aβ to form β-sheet structure in hydrophobic environments. The Aβ3pE−28 peptide forms particularly stable β-sheet structure in SDS micelles and in TFE. The fact that the Aβ28 pyroglutamyl peptides and the more hydrophobic Aβ40 pyroglutamyl peptides have a tendency to form β-sheet structure in both aqueous hydrophilic and membrane-like hydrophobic environments indicates that the increased aggregation propensity of these pyroglutamyl-containing peptides is not simply due to increased hydrophobicity.

The structural reasons for the greater propensity for β-sheet formation and deposition of pyroglutamyl peptides are not clear, especially as the structure of Aβ amyloid is not known. If the Aβ fibril is a hydrogen-bonded parallel β-sheet as previously suggested (*31*), then the loss of N-terminal charges may facilitate β-sheet formation by decreasing the level of unfavorable interstrand charge repulsion. Also, the loss of the two carboxylic acid functionalities from near the N-terminus, aspartic acid at position 1 and glutamic acid at position 3, may destabilize helix formation by eliminating favorable charge dipole interactions (*32*). However, this loss of stabilization would be at least partially offset by an increase in helical stability due to the loss of the unfavorable N-terminal positive charge. Therefore, it is likely that the increased aggregation propensity of the pyroglutamyl-containing peptides is a result of stabilized β-sheet formation, rather than a destabilization of α-helical structure.

It is not known whether the post-translational modifications that form Aβ3pE and Aβ11pE occur intracellularly and/or intercellularly (*14*). Secreted Aβ produced by cultured cells contained a number of N-terminal truncated peptides but no detectable pyroglutamyl forms (*33*). Although Aβ3pE appears to predate untruncated Aβ in plaque formation, no obvious protease or microglial activity correlates with its appearance (*34*) The formation of pyroglutamyl-containing Aβ peptides may be a direct result of early AD pathological processes. Because pyroglutamyl-containing Aβ variants both are abundant in AD brain and have a high propensity to aggregate, then the identification and inhibition of the mechanism of N-terminal truncation of full-length Aβ may be a potential therapeutic strategy for AD. At the very least, the presence of, and possible pathological role of, these pyroglutamyl forms of Aβ should be taken into account when studying Aβ depositability and in the development of bioassays for screening for aggregation inhibitors.

ACKNOWLEDGMENT

We thank Teck-Kwang Lim for some HPLC purifications, Andrew Thompson for help with some CD experiments, and Su-Ting Liu, Geoff Howlett, and Bill Sawyer for help with the sedimentation experiments. We also thank Andrew Clippingdale, Michael Jobling, Roberto Cappai, Robert Cherny, and Colin Masters for helpful discussion.

REFERENCES

1. Tanzi, R. E. (1989) *Ann. Med. 21*, 91−94.
2. Glenner, C. G. (1988) *Cell 52*, 307−308.
3. Masters, C. L., Simms, G., Weinman, N. A., Multhaup, C. G., McDonald, B. L., and Beyreuther, K. (1985) *Proc. Natl. Acad. Sci. U.S.A. 82*, 4245−4249.
4. Selkoe, D. J. (1993) *Trends Neurosci. 16*, 403−406.
5. Mullan, M., and Crawford, F. (1993) *Trends Neurosci. 16*, 398−403.
6. Kang, J., Lemaire, H. G., Unterbeck, A., Salbaum, J. M., Masters, C. L., Grzescik, K. H., Multhaup, G., Beyreuther, K., and Muller-Hill, B. (1987) *Nature 325*, 733−766.
7. Barrow, C. J., and Zagorski, M. G. (1991) *Science 253*, 179−182.
8. Barrow, C. J., Yasuda, A., Kenny, P., and Zagorski, M. G. (1992) *J. Mol. Biol. 225*, 1075−1093.
9. Zagorski, M. G., and Barrow, C. J. (1992) *Biochemistry 31*, 5621−5631.
10. Jarrett, J. T., and Lansbury, P. T., Jr. (1993) *Cell 73*, 1055−1058.
11. Yankner, B. A., Dawes, L. R., Fisher, S., Villa-Lormaroff, L., Oster-Granite, M. L., and Neve, R. L. (1989) *Science 245*, 417−420.
12. Roher, A. E., Lowenson, J. D., Clarke, S., Wolkow, C., Wang, R., Cotter, R. J., Reardon, I. M., Zurcher-Neely, H. A., Heinrikson, R. L., Ball, M. J., and Greenberg, B. D. (1993) *J. Biol. Chem. 268*, 3072−3083.
13. Kuo, Y.-M., Webster, S., Emmerling, M. R., Lima, N. D., and Roher, A. E. (1998) *Biochim. Biophys. Acta 1406*, 291−298.
14. Kuo, Y.-M., Emmerling, M. R., Woods, A. S., Cotter, R. J., and Roher, A. E. (1997) *Biochem. Biophys. Res. Commun. 237*, 1988−1991.
15. Iwatsubo, T., Saido, T. C., Mann, D. M., Lee V. M., and Trojanowski, J. Q. (1996) *Am. J. Pathol. 149*, 1823−1830.
16. Hosoda, R., Saido, T. C., Otvos, L., Jr., Arai, T., Mann, D. M., Lee, V. M., Trojanowski, J. Q., and Iwatsubo, T. (1998) *J. Neuropathol. Exp. Neurol. 57*, 1086−1095.
17. Saido, T. C., Iwatsubo, T., Mann, D. M. A., Shimada, H., Ihara, Y., and Kawashima, S. (1995) *Neuron 14*, 457−466.
18. Russo, C., Saido, T. C., DeBusk, L. M., Tabaton, M., Gambetti, P., and Teller, J. K. (1997) *FEBS Lett. 409*, 411−416.
19. Saido, T. C., Yamao-Harigaya, W., Iwatsubo, T., and Kawahima, S. (1996) *Neurosci. Lett. 215*, 173−176.
20. Szendrei, G. I., Prammer, K. V., Vasko, M., Lee, V. M., and Otvos, L., Jr. (1996) *Int. J. Pept. Protein Res. 47*, 289−296.
21. Alewood, D., Schnolzer, M., Alewood, P., Jones, A., and Kent, S. B. (1992) *Int. J. Pept. Protein Res. 40*, 180−193.
22. Kaiser, E., Colescott, R. L., Bossinger, C. D., and Cook, P. I. (1970) *Anal. Biochem. 34*, 595−598.
23. Pike, C. J., Walencewicz-Wasserman, A. J., Kosmoski, J., Cribbs, D. H., Glabe, C. G., and Cotman, C. W. (1995) *J. Neurochem. 64*, 253−265.
24. Greenfield, N., and Fasman, G. D. (1969) *Biochemistry 8*, 4108−4116.
25. Sticht, H., Bayer, P., Willbold, D., Dames, S., Hilbich, C., Beyreuther, K., Frank, R. W., and Rosch, P. (1995) *Eur. J. Biochem. 233*, 293−298.
26. Watson, A. A., Fairlie, D. P., and Craik, D. J. (1998) *Biochemistry 37*, 12700−12706.
27. Coles, M., Bicknell, W., Watson, A. A., Fairlie, D. P., and Craik, D. J. (1998) *Biochemistry 37*, 11064−11067.

28. Hollosi, M., Otvos, L., Jr., Kajtar, J., Percel, A., and Lee, V. M. (1989) *Pept. Res. 2*, 109−113.
29. Soto, C., Castano, E. M., Kumar, R. A., Beavis, R. C., and Frangione, B. (1995) *Neurosci. Lett. 200*, 105−108.
30. Fabian, H., Szendrei, G. I., Mantsch, H. H., Greenberg, B. D., and Otvos, L., Jr. (1994) *Eur. J. Biochem. 221*, 959−964.
31. Benzinger, T. L. S., Gregory, D. M., Burkoth, T. S., Miller-Auer, H., Lynn, D. G., Botto, R. E., and Meredith, S. C. (1998) *Proc. Natl. Acad. Sci. U.S.A. 95*, 13407−13412.
32. Houston, M. E., Jr., Campbell, A. P., Lix, B., Kay, C. M., Sykes, B. D., and Hodges, R. S. (1996) *Biochemistry 35*, 10041−10050.
33. Wang, R., Sweeney, D., Gandy, S. E., and Sisodia, S. S. (1996) *J. Biol. Chem. 271*, 31894−31900.
34. Mann, D. M. A., Iwatsubo, T., Fukumoto, H., Ihara, Y., Odaka, A., and Suzuki, N. (1995) *Acta Neuropathol. 90*, 472−477.

BI990563R